ACS APPLIED BIO MATERIALS

www.acsabm.org

Forum Article

Skin Tolerability of Oleic Acid Based Nanovesicles Designed for the Improvement of Icariin and Naproxen Percutaneous Permeation

Shabir Ahmad,[††] Nicola d'Avanzo,[††] Antonia Mancuso, Antonella Barone, Maria Chiara Cristiano, Cristina Carresi, Vincenzo Mollace, Christian Celia,* Massimo Fresta,* and Donatella Paolino*

Cite This: https://doi.org/10.1021/acsabm.4c00067

Read Online

ACCESS | Metrics & More | Article Recommendations | Supporting Information

ABSTRACT: Deformable nanovesicles have a crucial role in topical drug delivery through the skin, due to their capability to pass intact the stratum corneum and epidermis (SCE) and significantly increase the efficacy and accumulation of payloads in the deeper layers of the skin. Namely, lipid-based ultradeformable nanovesicles are versatile and load bioactive molecules with different physicochemical properties. For this reason, this study aims to make oleic acid based nanovesicles (oleosomes) for the codelivery of icariin and sodium naproxen and increase their permeation through the skin. Oleosomes have suitable physicochemical properties and long-term stability for a potential dermal or transdermal application. The inclusion of oleic acid in the lipid bilayer increases 3-fold the deformable properties of oleosomes compared to conventional liposomes and significantly improves the percutaneous permeation of icariin and sodium naproxen through the human SCE membranes compared to hydroalcoholic solutions of both drugs. The tolerability studies on human volunteers demonstrate that oleosomes are safer and speed up the recovery of transepidermal water loss (TEWL) baselines compared to saline solution. These results highlight promising properties of icariin/sodium naproxen coloaded oleosomes for the treatment of skin disorders and suggest the potential future applications of these nanovesicles for further *in vivo* experiments.

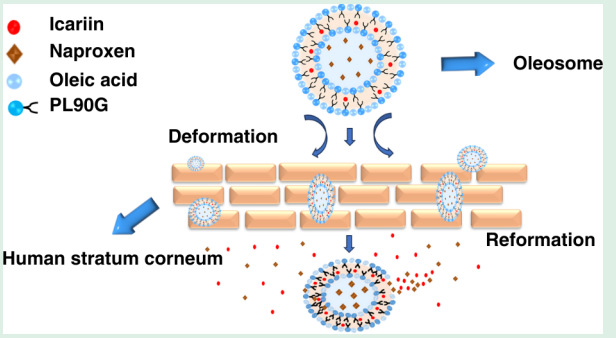

KEYWORDS: *oleosomes, icariin, sodium naproxen, nanovesicles, percutaneous permeation, skin tolerability, deformability index*

INTRODUCTION

Deformable lipid-based nanovesicles are significantly changing the scenario of topical skin drug delivery due to their capability to penetrate the stratum corneum and epidermis (SCE) and improve the accumulation of payloads in the deeper layers of the skin.[1−3]

We have previously demonstrated that by adding natural and synthetic surfactants, like sodium cholate derivatives,[4] ascorbyl palmitate,[5] and bola derivatives,[6] to the phospholipid mixture, we can have elastic liposomes that pass the SCE, accumulate drugs in the deeper layers of the skin, and increase the payload efficacy in animal models and human volunteers. In fact, the presence of surfactants favors the deformation of the resulting elastic liposomes that can squeeze by pore channels between tight junctions of the skin and permeate following the cutaneous aqueous gradient or modify the SCE structure and pass associated with payloads.[7] In these attempts, oleic acid based nanovesicles (oleosomes) may represent a viable option to improve the drug percutaneous permeation, by exploiting the intrinsic permeation enhancer properties of this fatty acid and deformable properties of the resulting nanovesicles.[8−10]

While the skin is the first barrier of the organism against pathogens and external insults, it is subject to several disorders,[11] and during the past few years the scientific community focused its attention on the use of natural compounds,[12,13] with or without delivery by nanocarriers,[14] as an alternative treatment to synthetic drugs. Among the different natural products that are currently used to treat dermatological diseases, Herba Epimedii, an herbaceous species, has been extensively used for many years by traditional Chinese medicine to treat different pathologies, including neurological and erectile dysfunctions, osteoporosis, and cardiac diseases.[15−18] Icariin (Ica) is the main flavonoid extracted from this plant, and it acts as a modulator of inflammation, also providing antioxidant and antiapoptotic effects.[19−21] Moreover, *in vivo* studies showed that Ica seems to promote wound healing through reducing pro-inflammatory cytokine production.[22,23] Although phytotherapeutics are efficacious *per se*, many research groups demonstrated that the combination between synthetic and plant-derived payloads can increase their therapeutic effects.[24,25] In this regard,

Special Issue: Early Career Forum 2024

Received: January 15, 2024
Revised: March 29, 2024
Accepted: April 2, 2024

naproxen (Npx) is a widely used nonsteroidal anti-inflammatory drug (NSAID), commercially available as a sodium derivative[26] but also loaded into many carriers, such as microemulsions, nanoemulsions, gels, and nanocarriers, to improve its percutaneous permeation.[27,28]

The aim of this study was to make an advanced drug delivery system and improve the skin percutaneous permeation of Npx and Ica, to provide a potential nanomedicine capable of combining the efficacies of both drugs for the treatment of disorders associated with skin inflammation. In these attempts, deformable nanovesicles were designed to enhance the passage of payloads through the skin.

This goal was achieved by adding oleic acid, which has a permeation enhancer property, into the bilayer of oleosomes. Moreover, the coloading of Ica and Npx into oleosomes, and the controlled drug release, may potentially increase the patient's compliance by decreasing the injected dosage and its frequency. These results, as well as biosafety and tolerability in healthy human volunteers, and the long-term stability of oleosomes, demonstrated that oleic acid made more deformable and stable nanovesicles than other natural and synthetic surfactants, and these elastic nanocarriers lay the bases for the potential application of Npx/Ica-coloaded oleosomes as a topical skin nanomedicine.

EXPERIMENTAL SECTION

Materials. Enriched soy phosphatidylcholine (Phospoliphon 90G, PL90G) was supplied by Lipoid GmbH (Ludwigshafen, Germany); phosphate-buffered saline (PBS) tablet, icariin (Ica; CAS No. 489-32-7), sodium naproxen (Npx; CAS No. 26159-34-2), oleic acid (99%), methanol (99.9%; CAS No. 67-56-1), and chloroform (CAS No. 67-66-3) were purchased from Sigma-Aldrich (St. Louis, MO, USA). All other reagents were of analytical grade and were used without further purification.

Oleosome Preparation. Oleosomes were prepared by the thin layer evaporation technique. PL90G and oleic acid (2:1 molar ratio) and icariin (at the proper amount to obtain a drug concentration of 1 mg/mL after the hydration step) were dissolved by using a methanol/chloroform (1:1 v/v) mixture in a Pyrex glass vial. The organic solvent was removed by a Rotavapor 210 (Büchi Italia, Milan, Italy) at 40 °C. The resulting lipid film was hydrated with 1 mg/mL sodium naproxen solution (PBS 10 mM, pH 7.4) by achieving a final lipid concentration of 20 mg/mL. Three alternating cycles of warming (45 °C) and vigorous vortex mixing (700 rpm) of 3 min each were carried out during the hydration process. The obtained colloidal suspension was kept in a water bath for 1 h at 45 °C to anneal the bilayer structure and then extruded using a Lipex extruder (Vancouver, Canada) at 45 °C through polycarbonate membrane filters ranging from 400 to 200 nm (Nuclepore polycarbonate membrane). The resulting Npx/Ica-coloaded oleosomes were purified by dialysis. Briefly, 1 mL of each sample was put in a cellulose membrane (cutoff 10 kDa) and allocated in 200 mL of receptor medium made up of a mixture of ethanol and PBS (3:7 v/v ratio) for 2 h to remove the not encapsulated drugs.

Physicochemical Characterization. Dynamic light scattering (DLS) analyses were used for the determination of the mean size and size distribution, expressed as a polydispersity index (PDI), of Npx/Ica-coloaded oleosome. A Zetasizer Nano ZS (Malvern Instruments, Worcestershire, U.K.), with a laser diode with 4.5 mV rated output, 670 nm wavelength, and 173° backscattering angle, was used for this characterization. The samples were diluted with an isotonic solution previously filtered through a polycarbonate membrane with an average pore size of 0.22 μm (Whatman Inc., Clifton, NJ, USA) to prevent the multiscattering phenomenon. In view of the oleosomes' electrophoretic mobility, the zeta potential value was also determined through the Zetasizer Nano ZS by using a Smoluchowsky constant $F(Ka)$ of 1.5.

Long-Term Stability Studies. As previously stated,[29] a Turbiscan Lab instrument was used to investigate the physical stability of the oleosomes. Oleosomes were diluted 10 times with PBS (10 mM, pH 7.4), held in a glass vial and analyzed at room (25 °C) and body (37 °C) temperatures. Studies were carried out by using an infrared light source (880 nm) and by recording the variation of transmitted (ΔT) and backscattered (ΔBS) light as a function of sample height and incubation time (1 h). The threshold of ±5% indicates the absence of destabilization phenomena. Analyses are reported in Results and Discussion for sample heights ranging between 2.5 and 10 mm. Variations in BS and T profiles, over this threshold at the sample height below 2 mm and over 10 mm, are not related to the occurrence of destabilization phenomena but are due to the bubble air at the liquid/glass and liquid/air interfaces, respectively. Furthermore, kinetic destabilization profiles of investigated samples were also recorded and reported as the Turbiscan stability index (TSI) vs incubation time (60 min).

To confirm the data obtained by using the Turbiscan Lab instrument, samples were stored at room temperature or at 4 °C up to 60 days. At fixed time points, i.e. 7, 30, and 60 days, the oleosomes' mean size and PDI were analyzed by DLS as described above.

Entrapment Efficiency and Release Kinetic Studies. After purification, the entrapped drugs were determined using an HPLC apparatus (Thermo Scientific, Rodano, MI, Italy) equipped with a UV detector. The samples were dried overnight by using a freeze-drying system (VirTis SP scientific sentry 2.0; SP Industries, Warminster, PA, USA) equipped with a vacuum pump (B14 model; Carpanelli S.p.a., Bologna, Italy) and then solubilized with methanol. This solution was suitably diluted and analyzed using a reverse phase C18 column (GreatSmart 15 cm × 4.6 mm, 5 μm). Drugs were eluted in a gradient mode using a formic acid (0.1% v/v) aqueous solution (phase A) and acetonitrile (ACN) as organic solvent (phase B) at a constant flow rate of 1 mL/min. The gradient was assessed as follows: 0−7 min 30% B; 7−7.1 min 40% B; 7.1−16 min 40% B; 16−16.1 min 30% B; 16−22 min 30% B. Chromeleon ver. 7 software was used to process the data. Determination was performed by using a proper external calibration curve for both Ica ($y = 0.493x + 0.0528$, $R^2 = 0.9989$) and Npx ($y = 6.1698x + 0.3294$, $R^2 = 0.9985$). The following equations were used to calculate the entrapment efficiency (EE, %) and drug loading (DL, %):

$$\text{EE}\ (\%) = D_e/D_{tot} \times 100 \quad (1)$$

$$\text{DL}\ (\%) = D_e/L_{tot} \times 100 \quad (2)$$

where D_e is the amount of encapsulated drug, while D_{tot} and L_{tot} are the total amounts of drug and lipids added during the preparation procedures, respectively.

A dialysis method was used to carry out the drugs' kinetic release studies from Ica/Npx-coloaded oleosome. Samples were placed into a dialysis membrane (molecular cutoff 10 kDa) clipped by standard closures and immersed into a suitable amount of receptor medium (PBS/ethanol mixture, 70:30 v/v), to reach a final sample/receptor medium ratio of 1:100 v/v. At specified time points, i.e., 30 mins and 1, 2, 3, 4, 6, 24, 48, and 72 h, 1 mL of the receptor medium was withdrawn and replaced with fresh buffer to maintain the sink conditions. The samples were gently magnetically stirred (200 rpm) for the entire analysis, and the temperature was maintained at 37 °C. The collected samples were analyzed by HPLC as described above.

Deformability Test. The deformability index (DI) of nanovesicles was evaluated by using a Lipex biomembranes extruder (Northern Lipids Inc., Vancouver, Canada). Briefly, Ica/Nxp-coloaded oleosome was extruded at room temperature through 50 nm pore size polycarbonate membrane filters at constant pressure of 5 bar for 10 min.[4] DI was calculated by using the following equation:

$$\text{DI} = J(d_0/p)[d_0/(d_0 - d_1)] \quad (3)$$

where J denotes the formulation fraction after extrusion, p is the pore size, and d_0 and d_1 are the average diameters of oleosomes before and after extrusion through a 50 nm filter, respectively.

https://doi.org/10.1021/acsabm.4c00067
ACS Appl. Bio Mater. XXXX, XXX, XXX−XXX

Percutaneous Permeation Studies. Franz diffusion vertical cells were used to evaluate the percutaneous permeation of Ica and Npx as free drugs or encapsulated into oleosomes. Human SCE membranes were isolated from skin sections obtained from surgical plastic reduction of healthy humans (mean age 31 ± 3) as previously reported.[10] Similarly to release experiments (Entrapment Efficiency and Release Kinetic Studies), the receptor fluid was a PBS/ethanol solution (70:30 v/v) warmed to 37 ± 2 °C, while the donor compartment was filled with 200 μL of sample. SCE membranes were placed between the donor and the receptor compartments of Franz cells with the stratum corneum layer facing the donor compartment, and at fixed time intervals 200 μL of the receptor media was withdrawn and replaced with the same amount of fresh media. The amount of ethanol in the receptor mixture, necessary to ensure sink conditions, elicited no significant alteration of the barrier function of human SCE membranes, as evaluated by transepithelial electrical resistance (TEER). The values of TEER have been kept below 2 kΩ for the entire experiments.[30] HPLC (see above) was used for the determination of the permeated drugs through SCE membranes. Percutaneous permeation rate of drug-loaded oleosomes was compared to the drug hydroalcoholic solution (PBS:ethanol v/v ratio). The study was carried out in accordance with the Declaration of Helsinki, and the procedures were authorized by the Research Ethics Committee of the University of Catanzaro "Magna Graecia" (Approval No. 390/2019).

Skin Tolerability Evaluation of Nanocarriers on Human Healthy Volunteers. For *in vivo* studies, 12 human healthy volunteers (both sexes with mean age 32 ± 5) were enrolled and appropriately informed about the nature of the study. After signing the informed consensus and approving the experimental protocol, the volunteers were accommodated for 1 h in a surgery room at controlled conditions of 24 ± 1 °C and 40−50% relative humidity.

The experimental protocol provided for the evaluation of transepidermal water loss (TEWL) by using the C+K Multi Probe Adapter with a Tewameter TM300 probe (Courage & Khazaka, Cologne, Germany). Two sites on both forearms (one for saline solution, used as negative control, and one for empty formulation) of each volunteer were marked using permanent ink, fixed at a distance between each site enough to avoid any type of interference. Commercial patches (Farmacosmo S.r.l., Napoli, Italy) for occlusive conditions were used to allow the application of 150 μL of each sample. At fixed times, the patches were gently removed from the skin and data (TEWL g/h·m^2) was collected by the Tewameter TM300 and processed by Courage & Khazaka MPA software.

The safety profile of oleosomes was further measured by using an X-Rite Ci62 (X-Rite Inc., Grandville, MI, USA). The variations of the skin color after topical application of oleosomes or saline solution were quantified up to 8 h in healthy volunteers that had been previously informed and signed the relative informed consent. Two chromophores (melanin and hemoglobin) were monitored during the study. Oleosomes and saline solution, as negative control, were applied on the forearm of human volunteers, and the variation of erythematous index (ΔEI) values with respect to the baseline of each site patch were calculated by using the following equation:

$$EI = 100[\log 1/R_{560} + 1.5(\log 1/R_{540} + \log 1/R_{580}) - 2(\log 1/R_{510}) + \log 1/R_{610})] \quad (4)$$

where $1/R$ is the inverse value of reflectance measured at different wavelengths (510, 540, 560, 580, 610 nm) depending on the hemoglobin and melanin absorbance.

In vivo studies were carried out in accordance with the Declaration of Helsinki, and the protocol was approved by the Research Ethics Committee of the University of Catanzaro "Magna Græcia" (Approval Nos.: 390/2019 and 392/2019).

Statistical Analysis. One-way analysis of variance (ANOVA) followed by *t*-test have been used to investigate the statistical significance. Three different significant levels have been used: *, $p < 0.05$; **, $p < 0.01$; ***, $p < 0.001$. Sigmaplot ver. 12 and Office 2010 were the software used to perform the statistical analysis.

RESULTS AND DISCUSSION

Physicochemical Characterization of Oleosomes. The goal of this study was to study the codelivery of Ica and Nxp by oleosomes and improve their skin percutaneous permeation.[31] The first investigative step was the evaluation of physicochemical properties of oleosomes and, in particular, whether the loading of Ica and/or Npx could modify the supramolecular structure and interface properties of the resulting nanovesicles. For this reason, empty, Npx-loaded, Ica-loaded, and Npx/Ica-coloaded oleosomes have been prepared and physicochemically characterized (Table 1).

Table 1. Oleosome Composition Summary

sample	lipid amt (mg/mL)	PL90G/oleic acid (molar ratio)	Npx (mg/mL)	Ica (mg/mL)
empty oleosomes	20	2:1	–	–
Npx-loaded oleosomes	20	2:1	1	–
Ica-loaded oleosomes	20	2:1	–	1
Npx/Ica-loaded oleosomes	20	2:1	1	1

Oleosomes were analyzed by DLS (Figure 1), and the resulting data showed suitable physicochemical properties for a

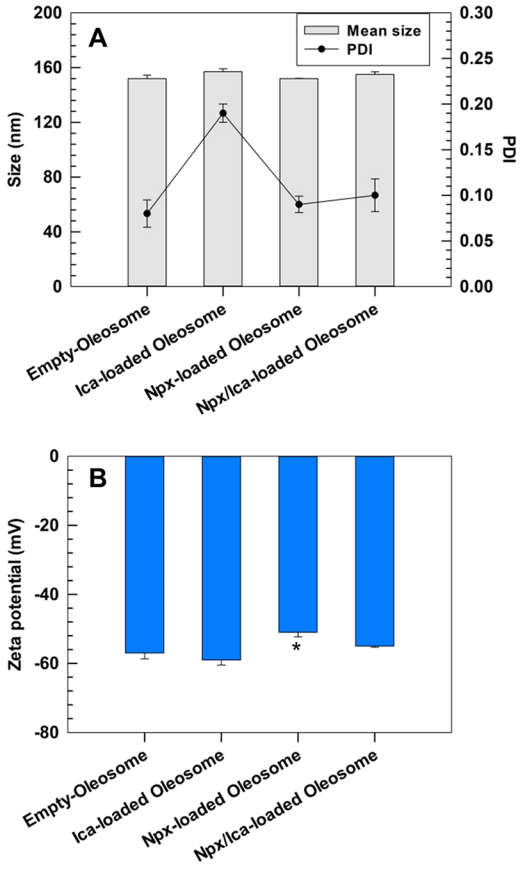

Figure 1. Physicochemical properties of empty oleosome, Ica-loaded oleosome, Npx-loaded oleosome, and Npx/Ica-coloaded oleosome. Panel A shows the mean size and the PDI values, while panel B reports the zeta potential of oleosomes. Results are the average of three independent experiments ± SD. Statistical significance was **, $p < 0.01$ (drug-loaded oleosomes vs empty oleosomes).

https://doi.org/10.1021/acsabm.4c00067
ACS Appl. Bio Mater. XXXX, XXX, XXX−XXX

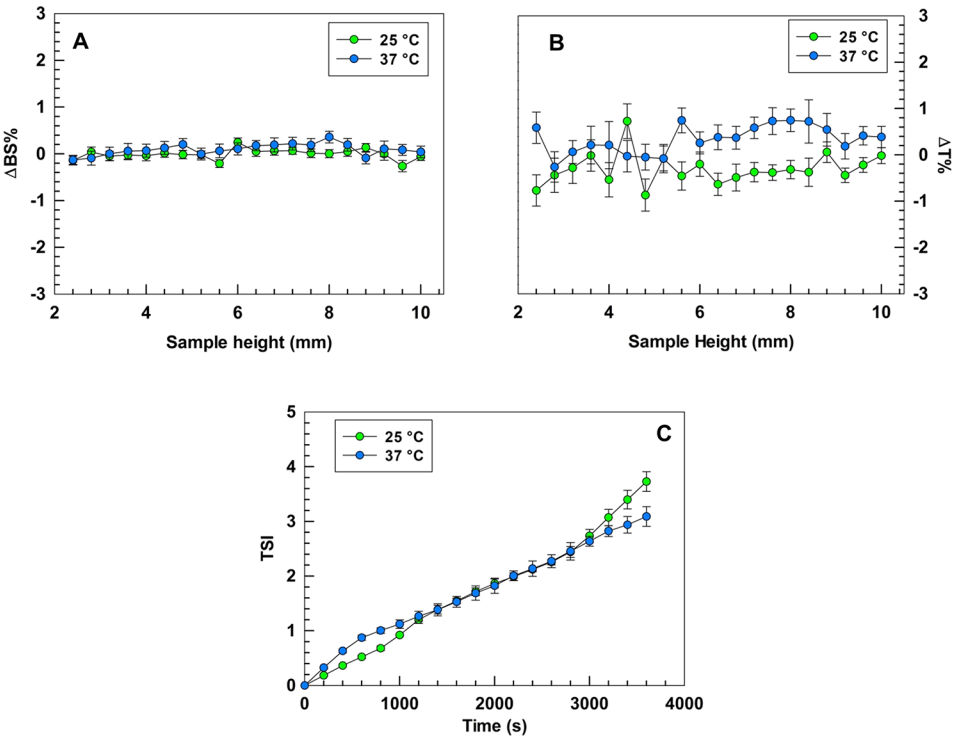

Figure 2. Turbiscan Lab analysis of Npx/Ica-coloaded oleosomes. Percentage variation of backscattering (ΔBS%) (A), percentage variation of transmission (ΔT%) (B), and Turbiscan Lab stability index (TSI) (C) were evaluated at 25 and 37 °C, as a function of sample height and incubation time (0−1 h). Results are the mean of three independent experiments ± SD.

potential topical skin application. In fact, the average size of ca. 160 nm allows the permeation of oleosomes through the skin,[32] while the PDI values less than or equal to 0.2 demonstrated a narrow size distribution.[33]

The presence of Npx or Ica, or both drugs, in oleosomes did not significantly modify the size or PDI, thus endorsing the lack of physical destabilization due to the drugs' loading. The zeta potential of oleosomes was below −50 mV for all the resulting nanovesicles due to the presence of the oleic acid carboxylic moiety on their surface, thus suggesting a proper electrostatic repulsion that stabilized oleosomes and prevented their aggregation in the dispersion medium.[34]

Npx-loaded oleosomes showed a reduction of the net zeta potential value compared to empty oleosomes, i.e., −57.0 ± 1.7 vs −51.0 ± 1.3, maybe due to the presence of Npx molecules adsorbed on the surface of oleosomes. Conversely, no statistical variations of the zeta potential value between empty and Npx/Ica-coloaded oleosomes or Ica-loaded oleosomes were obtained. Noteworthy, the presence of Ica in the oleosomes coloading the two drugs determined a similar zeta potential value to empty oleosomes, thus antagonizing the Npx effect. This result could depend on the partitioning of Ica in the lipid bilayer, thus leading to the exposure of different residuals on the nanovesicle surface.

Long-Term Stability Studies. As previously reported by our research group,[29] the Turbiscan Lab apparatus can predict the occurrence of destabilization phenomena by correlating the backscattered and transmitted light by and through the samples. In these attempts, Npx/Ica-coloaded oleosomes were analyzed at 25 and 37 °C, to mimic the room storage and body temperatures, respectively. No variation over ±5%, for backscattering (ΔBS) and transmission (ΔT), was recorded at both temperatures. The resulting data showed almost overlapped profiles, thus evidencing the physical stability of tested oleosomes.[4] ΔBS and ΔT signals of Npx/Ica-loaded oleosomes were in the range of ±2% (Figure 2), which is similar to other stable nanocarriers previously published,[35,36] thus demonstrating that the inclusion of oleic acid in the lipid bilayer did not modify the supramolecular structure of nanocarriers and did make stable nanoformulations. The analysis of TSI further confirmed the absence of destabilization phenomena at both room and body temperatures, by showing a similar trend of other stable deformable nanovesicles reported elsewhere.[4] The TSI value, combining the variation of backscattered and transmitted light, easily predicts the stability of colloidal nanovesicles and shows the sizes of nanovesicles that are directly related to physical destabilization phenomena without any dilution of the samples. The Turbiscan data, in agreement with the net negative charge of the zeta potential, further demonstrated that oleosomes are stable and the physical destabilization phenomena, like flocculation, sedimentation, or creaming, did not occur for the resulting nanovesicles before and after loading of payloads.

Similar results were obtained for both Ica-loaded oleosomes and Npx-loaded oleosomes (Figures S1 and S2), thus endorsing that the loading of both drugs into oleosomes did not destabilize the resulting nanovesicle formulation.

To confirm the physical stability of oleosomes, Npx/Ica-coloaded oleosomes were stored at 25 and 4 °C up to 60 days and then analyzed in terms of mean size and PDI at specific time points (Figure 3).

As demonstrated in Figure 3, no significant variation of mean size for Npx/Ica-coloaded oleosomes was observed at both incubation temperatures. Indeed, the Npx/Ica-coloaded oleosomes showed a slight and insignificant increase (ca. 10 nm) after 60 days of incubation, thus maintaining a mean size

https://doi.org/10.1021/acsabm.4c00067
ACS Appl. Bio Mater. XXXX, XXX, XXX−XXX

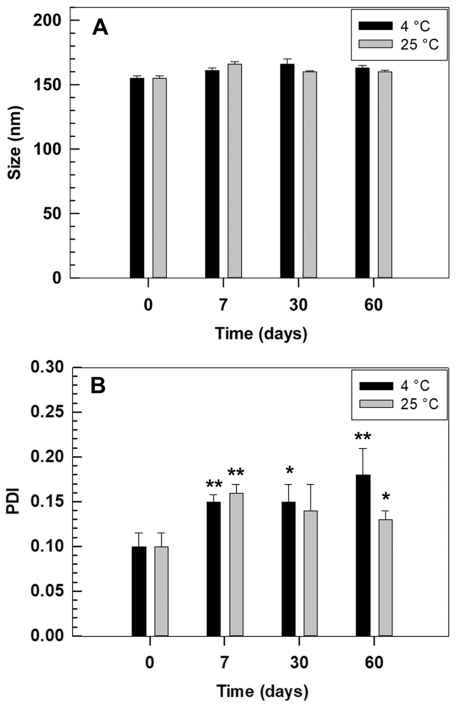

Figure 3. Long-term storage profiles of Npx/Ica-coloaded oleosomes as a function of time and temperature. Panel A reports the mean size of Npx/Ica-coloaded oleosomes, and panel B presents the PDI profiles at both temperatures. Results are the average of three independent experiments ± SD. Statistical significance was ∗, $p < 0.05$; ∗∗, $p < 0.01$; and (time 0 vs time points).

below 200 nm. PDI values also showed the preservation of a suitable size distribution profile for the full incubation time (values below 0.2).

Results obtained by Turbiscan Lab and DLS analyses demonstrated that suitable physicochemical properties of oleosomes were kept over time, regardless of the loading of payloads and the storage conditions, thus demonstrating a proper long-term stability of the investigated Npx/Ica-coloaded oleosomes, which is a crucial point for the preparation of a potential nanomedicine for skin topical drug delivery.

Entrapment Efficiency and Release Kinetic Profiles. Stable oleosomes were further studied for drug loading efficiency. Npx/Ica-coloaded oleosomes had entrapment efficiencies of 56.3 ± 2.2% and 67.5 ± 6.7% for Npx and Ica, respectively, and drug loadings of 2.8 ± 0.1% and 3.37 ± 0.3%, for Npx and Ica, respectively (Table 2). These results agreed with data previously published for other nanocarriers that are used for topical delivery of Npx[5] and/or other natural-derived lipophilic molecules.[37] The coloading of Ica and Npx into oleosomes did not affect the drug entrapment efficiency or loading degree compared to the single loading of the two drugs (Figure S3). This is due to the partitioning of selected drugs into the two different compartments of oleosomes, i.e., aqueous core and lipid bilayer for Npx and Ica, respectively.

Apart from the improved permeation of payloads through the skin, an ideal drug delivery system should guarantee a sustained and controlled release of the payload. Based on that, the release kinetic profiles of both drugs from Npx/Ica-coloaded oleosomes have been studied up to 72 h. Figure 4 shows a biphasic release of Npx and Ica with a pseudosteady state after 48 h incubation, which led to a final release rate of ∼80% of both payloads. Npx showed a significant burst release within the first 2 h of incubation compared to Ica. This trend might depend on the presence of Npx molecules adsorbed on the surface of oleosomes, thus endorsing our hypothesis discussed above. Moreover, almost 50% of Npx and Ica were released within the first 6 h, which is a suitable kinetic profile for a potential topical application.

Table 2. Entrapment Efficiency and Drug Loading Percentage of Npx/Ica-Coloaded Oleosomes[a]

	entrapment efficiency (%)	drug loading (%)
Npx	56.3 ± 2.2	2.8 ± 0.1
Ica	67.5 ± 6.7	3.4 ± 0.3

[a]Results are the average of three independent experiments ± SD.

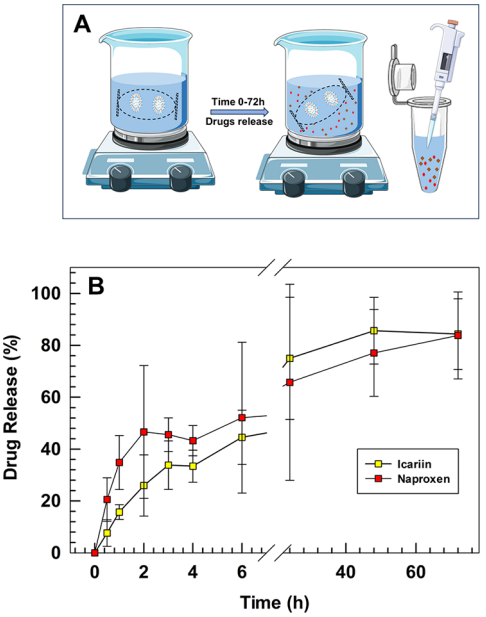

Figure 4. Kinetic release profiles of Ica and Npx. Panel A is a schematic representation of release experiments, while panel B shows the release rate (%) of both drugs as a function on the incubation time. Results are the average of three independent experiments ± SD.

Deformability Index. One of the main features required of a drug delivery system for a potential topical skin application is its deformation following the passage through the skin. This property preserves the integrity of payloads through the skin and the accumulation of cargos in the deepest skin layers.[38] The deformation of nanocarriers depends on penetration enhancers, like surfactants, that are part of the lipid bilayers and promote the squeezing of nanocarriers through the tight junctions among the cells or the intercalation of vesicles through the SCE membranes.[39] Oleic acid is a well-known penetration enhancer, and its inclusion in the lipid bilayer of nanovesicles improves their deformability.[40,41] To demonstrate this feature, we measured the deformability index of oleosomes by using the extrusion method[42,43] and compared it with that of liposomes, which are recognized as rigid lipid-based nanovesicles.[7] As reported in Figure 5, empty oleosomes showed a DI almost 3 times higher than empty liposomes (8.92 ± 0.05 and 3.19 ± 0.6, respectively). In particular, the oleosome DI value was similar to the value obtained in a

https://doi.org/10.1021/acsabm.4c00067
ACS Appl. Bio Mater. XXXX, XXX, XXX−XXX

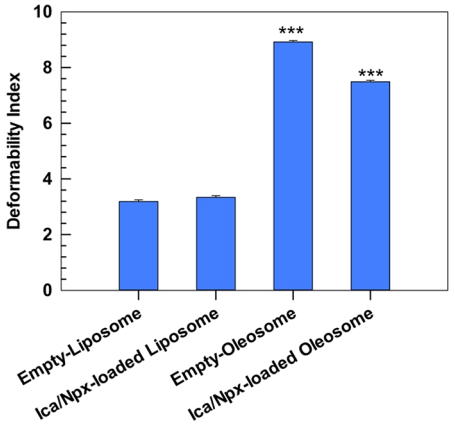

Figure 5. Deformability index of oleosomes and liposomes. Results are the average of three independent experiments ± SD. Statistical significance was ***, $p < 0.001$ (oleosomes vs liposomes).

previous study for transfersomes, which are considered one of the gold standard elastic/deformable vesicles for dermal and/or transdermal application.[4]

The coloading of Npx and Ica significantly reduced the DI of oleosomes. Conversely, no significant variations were observed when both drugs were coloaded into liposomes. Probably the more rigid structure of liposomes is not or is very poorly affected by the presence of cargos. However, despite the reduced DI of oleosomes due to the presence of payloads, Npx/Ica-coloaded oleosomes still showed a DI 2 times higher than liposomes, 7.49 ± 0.05 and 3.34 ± 0.06, respectively, thus still demonstrating suitable features to pass across the SCE and provide an effective accumulation of payloads in the deepest skin layer. A similar trend was carried out for Ica-loaded liposomes or oleosomes and Npx-loaded liposomes or oleosomes (Figure S4). No significant variation of DI was measured for Ica- or Npx-loaded liposomes compared to empty liposomes, while a slight decrease of DI (up to ca. 8) was carried out for Ica-loaded oleosomes and Npx-loaded oleosomes compared to empty liposomes and oleosomes. Differences may depend on the more elastic bilayer of oleosomes than liposomes affecting the loading of both hydrophobic and hydrophilic drugs, but it is independent of their physicochemical properties. In fact, the DI values for Ica-loaded oleosomes and Npx-loaded oleosomes are 8.06 ± 1.41 and 8.16 ± 0.09, respectively.

Permeation Studies. To confirm the efficacy of oleosomes as topical skin drug delivery systems, the percutaneous permeation studies were carried out by using human SCE membranes and Franz diffusion cells.[10] The percutaneous permeation of Npx/Ica-coloaded oleosomes was compared to conventional Npx/Ica hydro-alcoholic solution, with the same concentration of Npx and Ica that have been loaded inside the oleosomes.

Hydroalcoholic solutions of Ica and Npx slightly permeate through SCE within 8 h (Figure 6). These results were in agreement with data previously published and were probably related to the physicochemical properties of Npx[44] as well as the poor water solubility of Ica.[45] Conversely, oleosomes increased the permeation of Npx and Ica after 4 h of experiment (Figure 6). In fact, after an incubation of 6 h, oleosomes improved 6 times and 20 times the percutaneous permeation of Npx and Ica, respectively, compared to Npx and Ica hydroalcoholic solutions (Figure 6). This trend was also

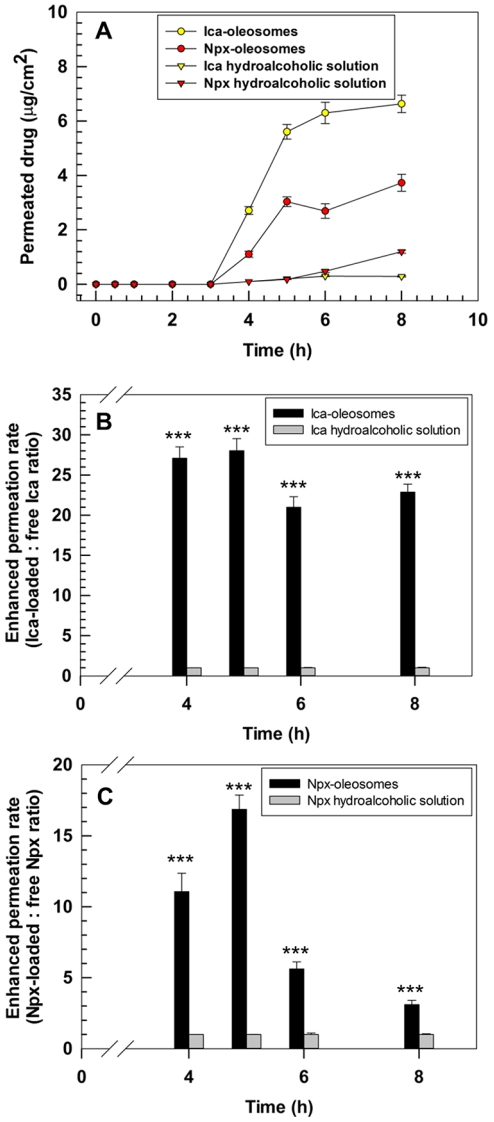

Figure 6. Percutaneous permeation of Npx/Ica-coloaded oleosomes and Npx/Ica hydroalcoholic solution as a function of incubation time. Panel A shows the kinetics of percutaneous permeation of free drugs and Npx/Ica-coloaded oleosomes, while panels B and C show the enhanced permeation rates of Ica/Npx-coloaded oleosomes compared with free drug hydroalcoholic solution. Results are the average of three independent experiments ± SD. Statistical significance was: ***, $p < 0.001$ (Ica/Npx-coloaded oleosomes vs drug hydroalcoholic solution).

maintained up to 8 h, and although the differences between free and encapsulated Npx permeation decreased at this time point, oleosomes still had the capability to increase 3-fold the amount of Npx permeated at this incubation time. No significant percutaneous permeation of free Ica was carried out after 8 h of incubation, probably due to its physicochemical properties which induced a high interaction rate with the lipid of SCE membranes.

These results support the hypothesis of proper interactions between lipid components of nanovesicles and those of SCE with a consequent improvement of skin permeation for drugs formulated as oleosomes.

***In Vivo* Tolerability Test on Human Volunteers.** One of the key parameters to be studied is the safety *per se* of optimized nanoformulations. In these attempts, oleosomes

https://doi.org/10.1021/acsabm.4c00067
ACS Appl. Bio Mater. XXXX, XXX, XXX−XXX

were tested on healthy human volunteers by measuring transepidermal water loss (TEWL) using a Tewameter TM30. TEWL can be considered an index of stratum corneum integrity since an increase in its value is correlated to a decreased skin's barrier function due to a widening of the skin junctions as a consequence of internal/external stress.[46] TEWL values are used both in pharmaceutical and cosmetic fields to test the tolerability of new topical products.[47] Hence, TEWL ($g/m^2 \cdot h$) profiles as a function of time are related to the safety properties of oleosomes (Figure 7A).

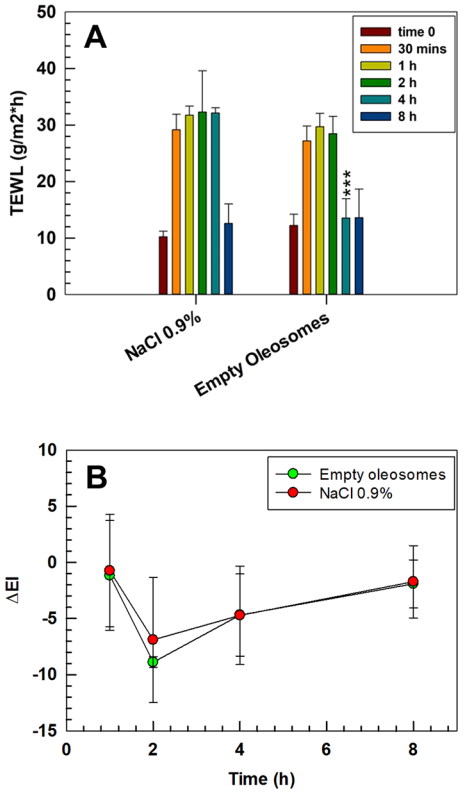

Figure 7. *In vivo* tolerability test. Panel A shows the TEWL induced by the application of oleosomes, while panel B reports the variation of the skin erythematous index (ΔEI). TEWL and ΔEI were studied on human volunteers as a function of time after topical application. NaCl solution (0.9% w/v) was used as negative control. The significant differences were evaluated for each time point by comparing the TEWL data of saline solution with that of oleosomes (***, $p < 0.001$). Results are the average of three independent experiments ± SD.

As reported in Figure 7A, a patch with saline solution (negative control) induced a reversible increase of TEWL values during the first 4 h. This trend is predictable and is due to the transient alteration of the skin hydration state induced on the application site by the patch.

Results showed that oleosomes neither altered the stratum corneum nor induced any irritation effect. Moreover, oleosomes speeded up the recovery of TEWL baseline values compared with the saline solution, maybe due to the lipid composition of oleosomes, which more effectively counteract the slight perturbation induced by the patch application. This finding not only endorsed the safety profiles of the resulting oleosomes but also demonstrated their capability to improve the skin functionality thanks to the hydrating effect of the lipid components.

The ΔEI of oleosomes was measured up to 8 h after their topical application to monitor the safety profile of nanovesicles. Oleosomes had similar values of ΔEI in the full range of analysis compared to saline solution (0.9% w/v NaCl) that had been used as control during the experiments (Figure 7B). Oleosomes, as well as the saline solution (control), had a skin whitening effect compared to the threshold analysis as demonstrated by the resulting negative values obtained up to 8 h of treatment (Figure 7B). The negative values of ΔEI obtained for oleosomes and saline solution may depend on the patch that has been used during the study. The lack of variations for ΔEI in human volunteers that have been topically treated with oleosomes further supported the results that have been obtained by TEWL analysis and endorsed the safety profile of oleosomes in human volunteers.

CONCLUSIONS

Oleosomes, oleic acid based nanovesicles, were studied for the topical skin delivery of icariin and sodium naproxen. Npx/Ica-coloaded oleosomes had suitable physicochemical properties for a potential topical application and skin delivery, i.e., a mean size of ca. 160 nm, a narrow size distribution (PDI below 0.2), and a zeta potential value below −50 mV. The presence of oleic acid in the main components of oleosomes significantly improved their deformability index compared to conventional liposomes, 7.49 ± 0.05 and 3.34 ± 0.06, respectively. Due to their high elasticity, after 6 h oleosomes improved 6 times and 20 times the percutaneous permeation of loaded Npx and Ica, respectively, compared to the free drug solutions after 6 h of application. Oleosomes can codeliver both natural and synthetic drugs, thus providing a potential nanomedicine able to combine the effect of both payloads. The sustained release profiles of oleosomes may increase the effectiveness of therapeutic drug dosage, decrease the frequency of injections, and thus improve the patients' compliance. Finally, the safety profiles of oleosomes in healthy human volunteers lay the perspective for further *in vivo* studies and support a potential use of oleosomes for the local treatment of skin disorders.

ASSOCIATED CONTENT

Supporting Information

The Supporting Information is available free of charge at https://pubs.acs.org/doi/10.1021/acsabm.4c00067.

Results of Turbiscan analysis of Ica-loaded oleosomes and Npx-loaded oleosomes; entrapment efficiency and drug loading degree of Ica-loaded oleosomes and Npx-loaded oleosomes; deformability index of Ica- and Npx-loaded liposomes or oleosomes (PDF)

AUTHOR INFORMATION

Corresponding Authors

Christian Celia − *Department of Pharmacy and UdA-TechLab, Research Center, University of Chieti−Pescara "G. d'Annunzio", 66100 Chieti, Italy; Laboratory of Drug Targets Histopathology, Institute of Cardiology, Lithuanian University of Health Sciences, LT-44307 Kaunas, Lithuania; Institute of Nanochemistry and Nanobiology, School of Environmental and Chemical Engineering, Shanghai University, Shanghai 200444, China;* orcid.org/0000-0002-0590-5429; Phone: +39 0871 3554711; Email: c.celia@unich.it

https://doi.org/10.1021/acsabm.4c00067
ACS Appl. Bio Mater. XXXX, XXX, XXX−XXX

Massimo Fresta − *Department of Health Sciences, University of Catanzaro "Magna Graecia", 88100 Catanzaro, Italy;* orcid.org/0000-0001-8062-817X; Phone: +39 0961 3694118; Email: fresta@unicz.it

Donatella Paolino − *Department of Experimental and Clinical Medicine, University of Catanzaro "Magna Graecia", 88100 Catanzaro, Italy; Research Center "ProHealth Translational Hub", Department of Experimental and Clinical Medicine, University of Catanzaro "Magna Graecia", 88100 Catanzaro, Italy*; Phone: +39 0961 3694211; Email: paolino@unicz.it

Authors

Shabir Ahmad − *Department of Health Sciences, University of Catanzaro "Magna Graecia", 88100 Catanzaro, Italy*

Nicola d'Avanzo − *Department of Experimental and Clinical Medicine, University of Catanzaro "Magna Graecia", 88100 Catanzaro, Italy; Research Center "ProHealth Translational Hub", Department of Experimental and Clinical Medicine, University of Catanzaro "Magna Graecia", 88100 Catanzaro, Italy*

Antonia Mancuso − *Department of Experimental and Clinical Medicine, University of Catanzaro "Magna Graecia", 88100 Catanzaro, Italy; Research Center "ProHealth Translational Hub", Department of Experimental and Clinical Medicine, University of Catanzaro "Magna Graecia", 88100 Catanzaro, Italy*

Antonella Barone − *Department of Experimental and Clinical Medicine, University of Catanzaro "Magna Graecia", 88100 Catanzaro, Italy*

Maria Chiara Cristiano − *Department of Medical and Surgical Sciences, University of Catanzaro "Magna Graecia", 88100 Catanzaro, Italy;* orcid.org/0000-0002-5510-7599

Cristina Carresi − *Institute of Research for Food Safety and Health IRC-FSH, Department of Health Sciences, University of Catanzaro "Magna Graecia", 88100 Catanzaro, Italy*

Vincenzo Mollace − *Institute of Research for Food Safety and Health IRC-FSH, Department of Health Sciences, University of Catanzaro "Magna Graecia", 88100 Catanzaro, Italy; Renato Dulbecco Institute, 88046 Catanzaro, Italy*

Complete contact information is available at: https://pubs.acs.org/10.1021/acsabm.4c00067

Author Contributions

[††]S.A. and N.d.A. contributed equally, and a purely alphabetical order is followed. Corresponding authors C.C., M.F., and D.P. contributed equally, and a purely alphabetical order is followed. The manuscript was written through contributions of all authors. All authors have given approval to the final version of the manuscript. S.A.: methodology, investigations, writing of original draft. N.d.A.: writing and review of original draft, data curation, formal analysis, investigation. M.F., D.P., C.C.: conceptualization, methodology, data curation, formal analysis, funding acquisition, writing—review and editing and supervision. A.M., A.B., M.C.C.: investigation, formal analysis and writing—review and editing. C.C.: investigation. V.M.: supervision and data analysis.

Funding

This work was funded by the Next Generation EU-Italian NRRP, Mission 4, Component 2, Investment 1.5, call for the creation and strengthening of "Innovation Ecosystems", building "Territorial R&D Leaders" (Directorial Decree no. 2021/3277)-project Tech4You-Technologies for climate change adaptation and quality of life improvement, no. ECS0000009. This work reflects only the authors' views and opinions; neither the Ministry for University and Research nor the European Commission can be considered responsible for them.

Notes

The authors declare no competing financial interest.

REFERENCES

(1) Sainaga Jyothi, V. G. S.; Ghouse, S. M.; Khatri, D. K.; Nanduri, S.; Singh, S. B.; Madan, J. Lipid nanoparticles in topical dermal drug delivery: Does chemistry of lipid persuade skin penetration? *J. Drug Delivery Sci. Technol.* **2022**, *69*, No. 103176.

(2) Ghasemiyeh, P.; Mohammadi-Samani, S. Potential of nanoparticles as permeation enhancers and targeted delivery options for skin: Advantages and disadvantages. *Drug Des. Dev. Ther.* **2020**, *14*, 3271−3289.

(3) Alexander, A.; Dwivedi, S.; Giri, T. K.; Saraf, S.; Saraf, S.; Tripathi, D. K.; Ajazuddin. Approaches for breaking the barriers of drug permeation through transdermal drug delivery. *J. Controlled Release* **2012**, *164* (1), 26−40.

(4) Cristiano, M. C.; d'Avanzo, N.; Mancuso, A.; Tarsitano, M.; Barone, A.; Torella, D.; Paolino, D.; Fresta, M. Ammonium glycyrrhizinate and Bergamot essential oil co-loaded ultradeformable nanocarriers: An effective natural nanomedicine for in vivo anti-inflammatory topical therapies. *Biomedicines* **2022**, *10* (5), 1039.

(5) d'Avanzo, N.; Cristiano, M. C.; Di Marzio, L.; Bruno, M. C.; Paolino, D.; Celia, C.; Fresta, M. Multidrug idebenone/naproxen co-loaded aspasomes for significant in vivo anti-inflammatory activity. *ChemMedChem* **2022**, *17* (9), No. e202200067.

(6) Cosco, D.; Paolino, D.; Muzzalupo, R.; Celia, C.; Citraro, R.; Caponio, D.; Picci, N.; Fresta, M. Novel PEG-coated niosomes based on bola-surfactant as drug carriers for 5-fluorouracil. *Biomed. Microdevices* **2009**, *11*, 1115−1125.

(7) Elsayed, M. M.; Abdallah, O. Y.; Naggar, V. F.; Khalafallah, N. M. Deformable liposomes and ethosomes: mechanism of enhanced skin delivery. *Int. J. Pharm.* **2006**, *322* (1−2), 60−66.

(8) Zakir, F.; Vaidya, B.; Goyal, A. K.; Malik, B.; Vyas, S. P. Development and characterization of oleic acid vesicles for the topical delivery of fluconazole. *Drug Delivery* **2010**, *17* (4), 238−248.

(9) Abdelalim, L. R.; Elnaggar, Y. S.; Abdallah, O. Y. Oleosomes encapsulating sildenafil citrate as potential topical nanotherapy for palmar plantar erythrodysesthesia with high ex vivo permeation and deposition. *AAPS PharmSciTech* **2020**, *21*, 310.

(10) Bruno, M. C.; Gagliardi, A.; Mancuso, A.; Barone, A.; Tarsitano, M.; Cosco, D.; Cristiano, M. C.; Fresta, M.; Paolino, D. Oleic acid-based vesicular nanocarriers for topical delivery of the natural drug thymoquinone: Improvement of anti-inflammatory activity. *J. Controlled Release* **2022**, *352*, 74−86.

(11) Ho, A. W.; Kupper, T. S. T cells and the skin: from protective immunity to inflammatory skin disorders. *Nat. Rev. Immunol.* **2019**, *19* (8), 490−502.

(12) Ijaz, S.; Akhtar, N.; Khan, M. S.; Hameed, A.; Irfan, M.; Arshad, M. A.; Ali, S.; Asrar, M. Plant derived anticancer agents: A green approach towards skin cancers. *Biomed. Pharmacother.* **2018**, *103*, 1643−1651.

(13) Merecz-Sadowska, A.; Sitarek, P.; Kucharska, E.; Kowalczyk, T.; Zajdel, K.; Cegliński, T.; Zajdel, R. Antioxidant properties of plant-derived phenolic compounds and their effect on skin fibroblast cells. *Antioxidants* **2021**, *10* (5), 726.

(14) Elhalmoushy, P. M.; Elsheikh, M. A.; Matar, N. A.; El-Hadidy, W. F.; Kamel, M. A.; Omran, G. A.; Elnaggar, Y. S. Elaboration of novel gel-core oleosomes encapsulating phytoconstituent for targeted topical delivery in a vitiligo-induced mouse model: Focus on antioxidant and anti-inflammatory pathways. *J. Drug Delivery Sci. Technol.* **2023**, *80*, No. 104119.

(15) Lu, Y.; Luo, Q.; Jia, X.; Tam, J. P.; Yang, H.; Shen, Y.; Li, X. Multidisciplinary strategies to enhance therapeutic effects of flavonoids from Epimedii Folium: Integration of herbal medicine, enzyme engineering, and nanotechnology. *J. Pharm. Anal.* **2023**, *13*, 239−254.
(16) Zhang, Y.; Ma, X.; Li, X.; Zhang, T.; Qin, M.; Ren, L. Effects of icariin on atherosclerosis and predicted function regulatory network in apoe deficient mice. *Biomed Res. Int.* **2018**, *2018*, 9424186.
(17) Ding, L.; Liang, X.-G.; Hu, Y.; Zhu, D.-Y.; Lou, Y.-J. Involvement of p38MAPK and reactive oxygen species in icariin-induced cardiomyocyte differentiation of murine embryonic stem cells in vitro. *Stem Cells Dev.* **2008**, *17* (4), 751−760.
(18) Sha, D.; Li, L.; Ye, L.; Liu, R.; Xu, Y. Icariin inhibits neurotoxicity of β-amyloid by upregulating cocaine-regulated and amphetamine-regulated transcripts. *Neuroreport* **2009**, *20* (17), 1564−1567.
(19) Jin, J.; Wang, H.; Hua, X.; Chen, D.; Huang, C.; Chen, Z. An outline for the pharmacological effect of icariin in the nervous system. *Eur. J. Pharmacol.* **2019**, *842*, 20−32.
(20) Fang, J.; Zhang, Y. Icariin, an anti-atherosclerotic drug from Chinese medicinal herb horny goat weed. *Front. Pharmacol.* **2017**, *8*, 734.
(21) Zhang, Y.; Wei, Y.; Zhu, Z.; Gong, W.; Liu, X.; Hou, Q.; Sun, Y.; Chai, J.; Zou, L.; Zhou, T. Icariin enhances radiosensitivity of colorectal cancer cells by suppressing NF-κB activity. *Cell Biochem. Biophys.* **2014**, *69*, 303−310.
(22) Huang, G.; Lin, Y.; Fang, M.; Lin, D. Protective effects of icariin on dorsal random skin flap survival: An experimental study. *Eur. J. Pharmacol.* **2019**, *861*, No. 172600.
(23) Singh, W. R.; Sharma, A.; Devi, H. S.; Bhatia, A.; Patel, M. R.; Kumar, D. Icariin improves cutaneous wound healing in streptozotocin-induced diabetic rats. *J. Tissue Viability* **2022**, *31* (1), 197−206.
(24) Postolović, K. S.; Antonijević, M. D.; Ljujić, B.; Radenković, S.; Miletić Kovačević, M.; Hiezl, Z.; Pavlović, S.; Radojević, I.; Stanić, Z. Curcumin and diclofenac therapeutic efficacy enhancement applying transdermal hydrogel polymer films, based on carrageenan, alginate and poloxamer. *Polymers* **2022**, *14* (19), 4091.
(25) Cosco, D.; Paolino, D.; Maiuolo, J.; Di Marzio, L.; Carafa, M.; Ventura, C. A.; Fresta, M. Ultradeformable liposomes as multidrug carrier of resveratrol and 5-fluorouracil for their topical delivery. *Int. J. Pharm.* **2015**, *489* (1−2), 1−10.
(26) Ramos, P.; Raczak, B. K.; Silvestri, D.; Wacławek, S. Application of TGA/c-DTA for Distinguishing between Two Forms of Naproxen in Pharmaceutical Preparations. *Pharmaceutics* **2023**, *15* (6), 1689.
(27) Martí-Centelles, R.; Dolz-Pérez, I.; De la O, J.; Ontoria-Oviedo, I.; Sepúlveda, P.; Nebot, V. J.; Vicent, M. J.; Escuder, B. Two-component peptidic molecular gels for topical drug delivery of naproxen. *ACS Appl. Bio Mater.* **2021**, *4* (1), 935−944.
(28) Anjum, F.; Zakir, F.; Verma, D.; Aqil, M.; Singh, M.; Jain, P.; Mirza, M. A.; Anwer, M. K.; Iqbal, Z. Exploration of nanoethosomal transgel of naproxen sodium for the treatment of arthritis. *Curr. Drug Del.* **2020**, *17* (10), 885−897.
(29) Celia, C.; Trapasso, E.; Cosco, D.; Paolino, D.; Fresta, M. Turbiscan Lab® Expert analysis of the stability of ethosomes® and ultradeformable liposomes containing a bilayer fluidizing agent. *Colloids Surf., B* **2009**, *72* (1), 155−160.
(30) Guth, K.; Schäfer-Korting, M.; Fabian, E.; Landsiedel, R.; Van Ravenzwaay, B. Suitability of skin integrity tests for dermal absorption studies in vitro. *Toxicol. In Vitro* **2015**, *29* (1), 113−123.
(31) Phatale, V.; Vaiphei, K. K.; Jha, S.; Patil, D.; Agrawal, M.; Alexander, A. Overcoming skin barriers through advanced transdermal drug delivery approaches. *J. Controlled Release* **2022**, *351*, 361−380.
(32) Rapalli, V. K.; Tomar, Y.; Sharma, S.; Roy, A.; Singhvi, G. Apremilast loaded lyotropic liquid crystalline nanoparticles embedded hydrogel for improved permeation and skin retention: An effective approach for psoriasis treatment. *Biomed. Pharmacother.* **2023**, *162*, No. 114634.
(33) Hoseini, B.; Jaafari, M. R.; Golabpour, A.; Momtazi-Borojeni, A. A.; Karimi, M.; Eslami, S. Application of ensemble machine learning approach to assess the factors affecting size and polydispersity index of liposomal nanoparticles. *Sci. Rep.* **2023**, *13* (1), 18012.
(34) Yu, H.-P.; Liu, F.-C.; Umoro, A.; Lin, Z.-C.; Elzoghby, A. O.; Hwang, T.-L.; Fang, J.-Y. Oleic acid-based nanosystems for mitigating acute respiratory distress syndrome in mice through neutrophil suppression: how the particulate size affects therapeutic efficiency. *J. Nanobiotechnology* **2020**, *18*, 25.
(35) Wang, Z.-Y.; Zhang, H.; Yang, Y.; Xie, X.-Y.; Yang, Y.-F.; Li, Z.; Li, Y.; Gong, W.; Yu, F.-L.; Yang, Z.; et al. Preparation, characterization, and efficacy of thermosensitive liposomes containing paclitaxel. *Drug Delivery* **2016**, *23* (4), 1222−1231.
(36) Tai, K.; Liu, F.; He, X.; Ma, P.; Mao, L.; Gao, Y.; Yuan, F. The effect of sterol derivatives on properties of soybean and egg yolk lecithin liposomes: Stability, structure and membrane characteristics. *Food Res. Int.* **2018**, *109*, 24−34.
(37) Elgewelly, M. A.; Elmasry, S. M.; El Sayed, N. S.; Abbas, H. Resveratrol-Loaded Vesicular Elastic Nanocarriers Gel in Imiquimod-Induced Psoriasis Treatment: In Vitro and In Vivo Evaluation. *J. Pharm. Sci.* **2022**, *111* (2), 417−431.
(38) Hallan, S. S.; Sguizzato, M.; Mariani, P.; Cortesi, R.; Huang, N.; Simelière, F.; Marchetti, N.; Drechsler, M.; Ruzgas, T.; Esposito, E. Design and characterization of ethosomes for transdermal delivery of caffeic acid. *Pharmaceutics* **2020**, *12* (8), 740.
(39) Cosco, D.; Celia, C.; Cilurzo, F.; Trapasso, E.; Paolino, D. Colloidal carriers for the enhanced delivery through the skin. *Expert Opin. Drug Delivery* **2008**, *5* (7), 737−755.
(40) Srisuk, P.; Thongnopnua, P.; Raktanonchai, U.; Kanokpanont, S. Physico-chemical characteristics of methotrexate-entrapped oleic acid-containing deformable liposomes for in vitro transepidermal delivery targeting psoriasis treatment. *Int. J. Pharm.* **2012**, *427* (2), 426−434.
(41) Rowat, A. C.; Kitson, N.; Thewalt, J. L. Interactions of oleic acid and model stratum corneum membranes as seen by 2H NMR. *Int. J. Pharm.* **2006**, *307* (2), 225−231.
(42) Costanzo, M.; Esposito, E.; Sguizzato, M.; Lacavalla, M. A.; Drechsler, M.; Valacchi, G.; Zancanaro, C.; Malatesta, M. Formulative study and intracellular fate evaluation of ethosomes and transethosomes for vitamin D3 delivery. *Int. J. Mol. Sci.* **2021**, *22* (10), 5341.
(43) Cristiano, M. C.; Barone, A.; Mancuso, A.; Torella, D.; Paolino, D. Rutin-loaded nanovesicles for improved stability and enhanced topical efficacy of natural compound. *J. Funct. Biomater.* **2021**, *12* (4), 74.
(44) Shah, H.; Nair, A. B.; Shah, J.; Jacob, S.; Bharadia, P.; Haroun, M. Proniosomal vesicles as an effective strategy to optimize naproxen transdermal delivery. *J. Drug Delivery Sci. Technol.* **2021**, *63*, No. 102479.
(45) Pikosz, K.; Nowak, I.; Feliczak-Guzik, A. Potential of Icariin−Glucosamine Combination in the Treatment of Osteoarthritis by Topical Application: Development of Topical Formulation and In Vitro Permeation Study. *Cosmetics* **2023**, *10* (1), 36.
(46) El-Chami, C.; Foster, A.; Johnson, C.; Clausen, R. P.; Cornwell, P.; Haslam, I.; Steward, M.; Watson, R.; Young, H.; O'Neill, C. Organic osmolytes increase expression of specific tight junction proteins in skin and alter barrier function in keratinocytes. *Br. J. Dermatol.* **2021**, *184* (3), 482−494.
(47) Stettler, H.; de Salvo, R.; Olsavszky, R.; Nanu, E. A.; Dumitru, V.; Trapp, S. Performance and tolerability of a new topical dexpanthenol-containing emollient line in subjects with dry skin: Results from three randomized studies. *Cosmetics* **2021**, *8* (1), 18.

https://doi.org/10.1021/acsabm.4c00067
ACS Appl. Bio Mater. XXXX, XXX, XXX−XXX